Ionics (2016) 22:2021–2026
DOI 10.1007/s11581-016-1750-x

ORIGINAL PAPER

Improved cycling performance of $LiNi_{0.8}Co_{0.15}Al_{0.05}O_2/Al_2O_3$ with core-shell structure synthesized by a heterogeneous nucleation-and-growth process

Gaole Dai[1] · Min Yu[1] · Fei Shen[1] · Jiali Cao[1] · Liang Ni[1] · Yanbin Chen[2] · Yuefeng Tang[1,3] · Yanfeng Chen[1]

Received: 5 May 2016 / Revised: 1 June 2016 / Accepted: 1 June 2016 / Published online: 11 June 2016

Abstract Al_2O_3 was successfully coated on $LiNi_{0.8}Co_{0.15}Al_{0.05}O_2$ cathode material by a heterogeneous nucleation-and-growth process with a core-shell structure for Li-ion battery. X-ray diffraction (XRD) measurements were used to indicate that the crystal structure of $LiNi_{0.8}Co_{0.15}Al_{0.05}O_2$ had no changes and no impurity phase existed after coating. Scanning electron microscopy (SEM) showed differences of surface morphology between coated and uncoated samples. A thin and bright coating layer was visually observed through transmission electron microscope (TEM). It reveals that the thickness of coating layer is 7 nm approximately. Electrochemical measurements were also carried out. Although the initial discharge capacity of the coated sample decreased, the 1-wt.% Al_2O_3-coated sample showed improved cycling performance at room temperature (25 °C) and elevated temperature (55 °C). It provided higher capacity retention of 71.7 and 70.1 % for 1C at 25 and 55 °C after 100 cycles, in comparison with 55.3 and 55.8 % for the uncoated sample. Meanwhile, interfacial resistance between active material and electrolyte decreased detected by electrochemical impedance spectroscopy (EIS) test. These enhancements in electrochemical characterizations are attributed to the improved stability of interface and the coating layer which served as the physical barriers to protect the active material from electrolyte attack.

Keywords Core-shell · $LiNi_{0.8}Co_{0.15}Al_{0.05}O_2$/Al2O3 · A heterogeneous nucleation-and-growth process · Lithium ion battery

Introduction

Nickel-rich cathode material $LiNi_{0.8}Co_{0.15}Al_{0.05}O_2$ is one of the most applicable cathode materials for advanced lithium ion batteries (LIBs). It has been widely used as power source for electric vehicles (EVs), hybrid electric vehicles (HEVs), and plug-in hybrid electric vehicles (PHEVs), due to its high energy, power density, and lower price [1–4]. However, there are some shortcomings, such as rapid capacity fading especially due to chemical instability of abundant Ni^{3+} and Ni^{4+} ions and its instability of structure at highly delithiated status and elevated temperature [5–8]. The appearance of abundant Ni^{4+} ions aggravates the side reaction between electrode and electrolyte, increases the impedance because of formation of solid electrolyte interface (SEI) layer, and lowers the cycling performance of LIBs [9–11]. In addition, LiOH impurities form on the surface of nickel-rich cathode material, react with $LiPF_6$ electrolyte, and yield HF which dissolves metal ions [12–14].

Many studies have indicated that it is a promising approach to improve the thermal stability and cycling stability of cathode materials of the nickel (Ni)-rich cathode material by coating of various materials. These coating materials can (i) act as a physical barrier, provide coated materials from HF attack, and thus reduce metal

✉ Yuefeng Tang
yftang@nju.edu.cn

[1] National Laboratory of Solid State Microstructures, College of Engineering and Applied Sciences, Nanjing University, Nanjing, Jiangsu 210093, China

[2] National Laboratory of Solid State Microstructures, School of Physics, Nanjing University, Nanjing 210093, China

[3] SuZhou Sun Sources Nano Science and Technology Co. Ltd, SuZhou, China

dissolution from the active materials to improve the surface stability of coated material; (ii) reduce side reactions between the electrode and the electrolyte; and (iii) enhance the capacity and electronic conductivity for some active coating materials [15]. For layered cathodes, metal oxides (SiO_2 [16], ZrO_2 [17, 18], and TiO_2 [19, 20]), metal fluorides (AlF_3 [21]), and metal phosphates ($AlPO_4$ and $Co_3(PO4)_2$ [22]) are suggested as suitable coating materials. For much cheaper price and more stable physical properties, Al_2O_3 coatings have been reported widely in previous references [12, 23, 24].

In this paper, Al_2O_3 was coated on $LiNi_{0.8}Co_{0.15}Al_{0.05}O_2$ cathode material via a heterogeneous nucleation-and-growth process [25–28] successfully. It is found that the cycling performance of Al_2O_3-coated cathode material was highly improved at high current intensity. In addition, the physical and electrochemical characterizations of the coated samples are discussed.

Experimental

Preparation of Al_2O_3-coated samples

$LiNi_{0.8}Co_{0.15}Al_{0.05}O_2$ was synthesized by co-precipitation method [29] as both the base material for coating and uncoated reference material. To prepare Al_2O_3-coated samples, $LiNi_{0.8}Co_{0.15}Al_{0.05}O_2$ powders were dispersed in aluminum isopropoxide ethanol solution with stirring vigorously for 5 h and evaporated at 60 °C subsequently to remove ethanol. The mixture was exposed in air with hydrolysis of aluminum isopropoxide to form film of gel on the surface of $LiNi_{0.8}Co_{0.15}Al_{0.05}O_2$ particles. And then particles were heated in air at 500 °C for 3 h in Muffle oven to obtain the Al_2O_3-coated $LiNi_{0.8}Co_{0.15}Al_{0.05}O_2$ materials. Amounts of Al_2O_3 were in the range 0.5 to 2 wt.%, and we denote the coating amounts of 0.5, 1, and 2 wt% as Al_2O_3-05, Al_2O_3-10, and Al_2O_3-20 respectively.

Physical characterization

The crystal structures of the samples were identified by X-ray diffraction (XRD) with Cu Kα radiation (ULTIMA-3, Rigaku, Japan), operated at 40 kV and 40 mA. The morphology and size of the samples was observed by field-emission scanning electron microscopy equipped with an EDXS energy disperse X-ray spectrometer (FESEM, Ultra55, Zeiss, Germany). Transmission electron microscopy (TEM, JEM-2100, JEOL) was taken to observe the coating layer. The quantitative atomic compositions and element valence of Al_2O_3-coated samples were determined by X-ray photoelectron spectroscopy (XPS, K-Alpha, Thermo Scientific, UK).

Electrochemical measurements

The cathode materials were mixed with acetylene black and polyvinylidene fluoride (PVDF) with a weight ratio of 80:10:10 in N-methyl-2-pyrrolidone (NMP). The slurry was coated on Al foil and dried in vacuum oven at 120 °C for 8 h. And then, the coin-type cell (CR2032) was assembled in a glove box (MBRAUN, Germany) filled with Ar, using lithium foil as the counter electrode, Celgard 2300 as the separator, and 1 M $LiPF_6$ in ethylene carbonate and dimethyl carbonate (1:1) as the electrolyte. The electrochemical performances were evaluated by electrochemical test instrument (Maccor S4000, USA) at different current densities in a voltage range of 2.8–4.5 V. The electrochemical impedance spectroscopy (EIS) measurement was carried out using an electrochemical

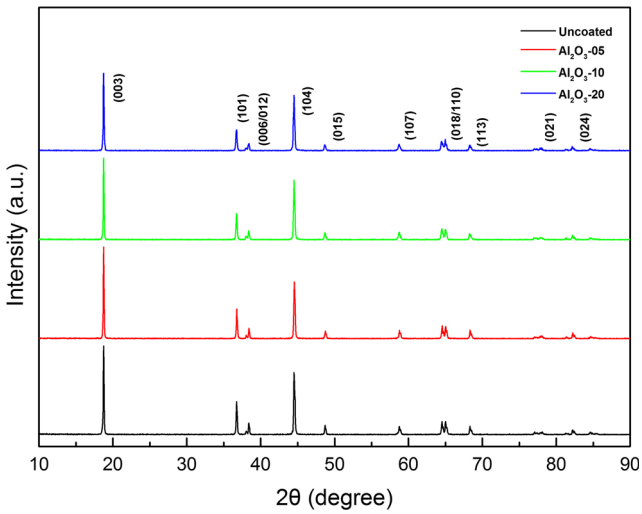

Fig. 1 XRD patterns of the uncoated and Al_2O_3-coated $LiNi_{0.8}Co_{0.15}Al_{0.05}O_2$: uncoated (**a**), Al_2O_3-05 (**b**), Al_2O_3-10 (**c**), and Al_2O_3-20 (**d**)

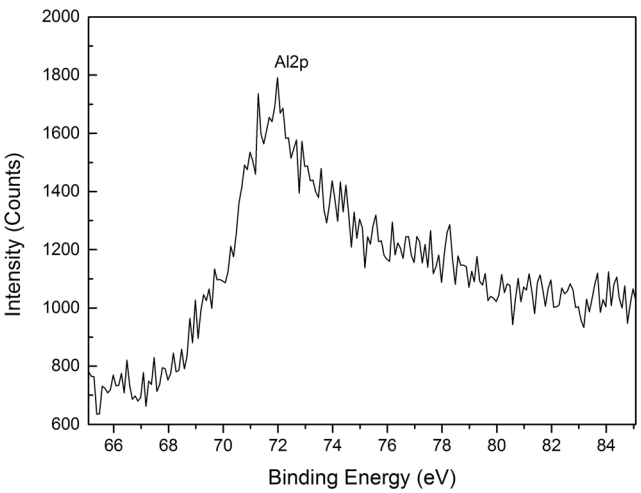

Fig. 2 XPS spectrum of Al2p taken from the surface of Al_2O_3-coated $LiNi_{0.8}Co_{0.15}Al_{0.05}O_2$ (Al_2O_3-10)

workstation (Solartron 1287, USA) over a frequency range from 10 mHz to 100 kHz with a 5-mV voltage vibration in order to detect the cell resistances at different cycle stages.

Result and discussion

XRD patterns and Miller indices of the uncoated and Al_2O_3-coated $LiNi_{0.8}Co_{0.15}Al_{0.05}O_2$ material are shown in Fig. 1. The crystal structure of the samples and all the diffraction peaks are in good agreement with the patterns of $LiNiO_2$ (JCPDS No. 74-0919) which reveals a single phase of α-$NaFeO_2$ structure with space group of R-3 m. Calculated by software Jade, the average crystal lattice constants are $a = 0.2868$ nm, $c = 1.4177$ nm for the uncoated sample with only a slight increase in the crystal constants, compared with $a = 0.2868$ nm, $c = 1.4186$ nm for the coated one. All these results suggest that the crystal structure of $LiNi_{0.8}Co_{0.15}Al_{0.05}O_2$ is not affected by coating. The splitting of the (006)/ (012) and (108)/ (110) peaks as well as the integrated ratios of I (003)/I (104) > 1.2 indicate the well-ordered α-$NaFeO_2$ structure with the limited cation mixing for both the bare and coated samples [30]. It can be indicated that the coating layer was nicely formed through a heterogeneous nucleation-and-growth process.

In order to clarify the oxidation state of Al in the Al_2O_3-coated samples, XPS analysis was performed at room temperature. XPS analysis of the coated sample (Al_2O_3-10) was carried out, and the Al2p XPS spectrum is given in Fig. 2. In this figure, the observed binding energy of the Al2p is 72.0 eV, which is very close to the values of 72.9 eV for Al_2O_3 (1999 XPS International, Inc.). This result shows that the Al element on the material surface is trivalent.

The surface morphologies of the uncoated and Al_2O_3-coated $LiNi_{0.8}Co_{0.15}Al_{0.05}O_2$ samples observed by SEM are shown in Fig. 3a, b. There are obvious differences in surface morphologies between the uncoated and Al_2O_3-coated $LiNi_{0.8}Co_{0.15}Al_{0.05}O_2$ samples. Plenty of nanometer primary particles are attached to the surface of secondary particles, as shown in Fig. 3a. After coating Al_2O_3 on the surface, primary particles of $LiNi_{0.8}Co_{0.15}Al_{0.05}O_2$ vanish with a few Al_2O_3 particles occurring indicating the Al_2O_3-coating layer is formed on the surface of the $LiNi_{0.8}Co_{0.15}Al_{0.05}O_2$ samples. The average diameter of $LiNi_{0.8}Co_{0.15}Al_{0.05}O_2$ particles is 7 μm. Also, the distribution of the four elements is revealed by a mapping of a single Al_2O_3-coated particle (Fig. 3c). SEM-EDS spectrum (Fig. 3d) shows O, Ni, Co, and Al characteristic peaks. According to atomic percentages of Ni, Co, and Al, the weight percentages of Al_2O_3 coated on the particle is 0.96 wt%.

Fine particles can provide nucleation centers, and can decrease the kinetic barrier to nucleation of a supersaturated solution. In this experiment, $LiNi_{0.8}Co_{0.15}Al_{0.05}O_2$ was used as nucleation centers in a supersaturated alumina sol suspension, so alumina sol can form a homogeneous layer on $LiNi_{0.8}Co_{0.15}Al_{0.05}O_2$ cores by the heterogeneous nucleation-and-growth processing. Transmission electron micrographs of the uncoated and Al_2O_3-coated $LiNi_{0.8}Co_{0.15}Al_{0.05}O_2$ powders (Al_2O_3-10) are shown in Fig. 4. By comparing morphology pictures of the uncoated

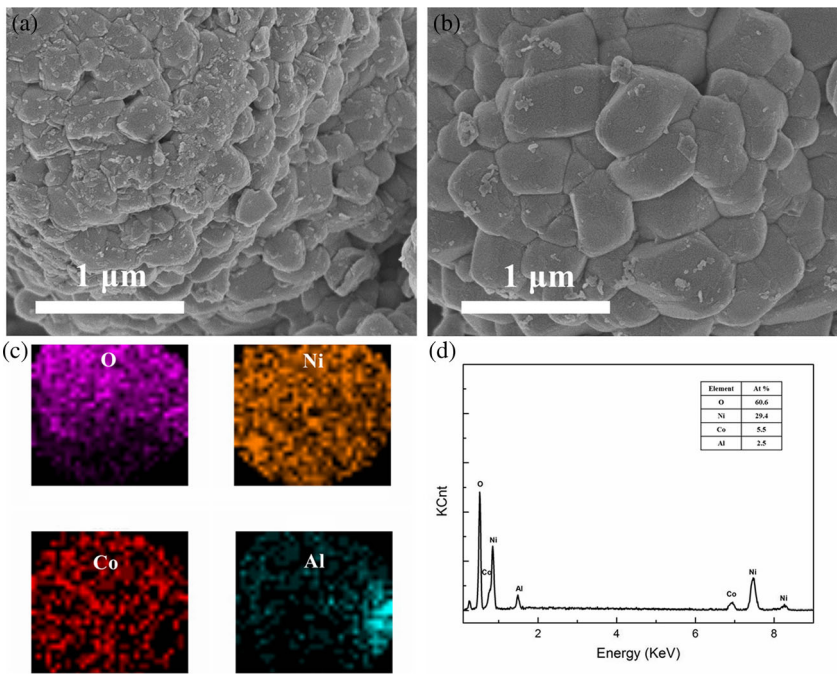

Fig. 3 SEM micrograph of the uncoated $LiNi_{0.8}Co_{0.15}Al_{0.05}O_2$ (**a**), SEM micrograph of the 1 wt.% Al_2O_3-coated $LiNi_{0.8}Co_{0.15}Al_{0.05}O_2$ (**b**), elemental mapping recorded from 1 wt.% Al_2O_3-coated $LiNi_{0.8}Co_{0.15}Al_{0.05}O_2$ with corresponding mappings of different elements (**c**), and EDS pattern of 1 wt.% Al_2O_3-coated $LiNi_{0.8}Co_{0.15}Al_{0.05}O_2$ (**d**)

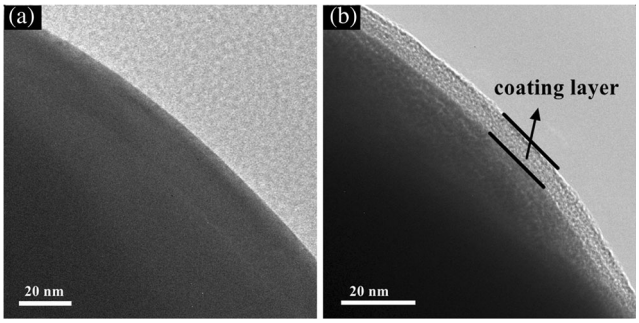

Fig. 4 TEM micrographs of the uncoated and Al_2O_3-coated $LiNi_{0.8}Co_{0.15}Al_{0.05}O_2$: uncoated (**a**) and Al_2O_3-10 (**b**)

samples with a clean and smooth surface in Fig. 4a, a thin and brighter coating layer is visually observed in Fig. 4b. It reveals that the thickness of coating layer is 7 nm approximately. Based on these facts, we confirm that a uniform surface coating of Al_2O_3 particles was successfully achieved.

Figure 5a shows initial charge–discharge curves of the Li/uncoated and Li/Al_2O_3-coated $LiNi_{0.8}Co_{0.15}Al_{0.05}O_2$ cells at a current density of 18 mA g^{-1} (0.1C) between 2.8 and 4.5 V. All the similar charge–discharge curves imply that no change of structure occurred through the process of Al_2O_3 coating. The initial discharge capacities of the uncoated and Al_2O_3-coated $LiNi_{0.8}Co_{0.15}Al_{0.05}O_2$ materials (Al_2O_3-05, Al_2O_3-10, and Al_2O_3-20) are 202.83, 199.21, 189.86, and 184.70 mAh g^{-1}, respectively. The capacities of the Al_2O_3-coated $LiNi_{0.8}Co_{0.15}Al_{0.05}O_2$ materials are lower than those of the uncoated material, which are on account of the existence of the inactive Al_2O_3 coated on the surface. Although the inactive Al_2O_3 coated on the surface decreases the initial discharge capacities of cells, the cyclability of 1-wt.% Al_2O_3-coated $LiNi_{0.8}Co_{0.15}Al_{0.05}O_2$ cells increases at the current rate of 180 mA g^{-1} (1C) between 2.8 and 4.5 V at room temperature (25 °C) and elevated temperature (55 °C) as shown in Fig. 5b, c. The discharge capacity at 25 and 55 °C of the uncoated $LiNi_{0.8}Co_{0.15}Al_{0.05}O_2$ materials decreases from

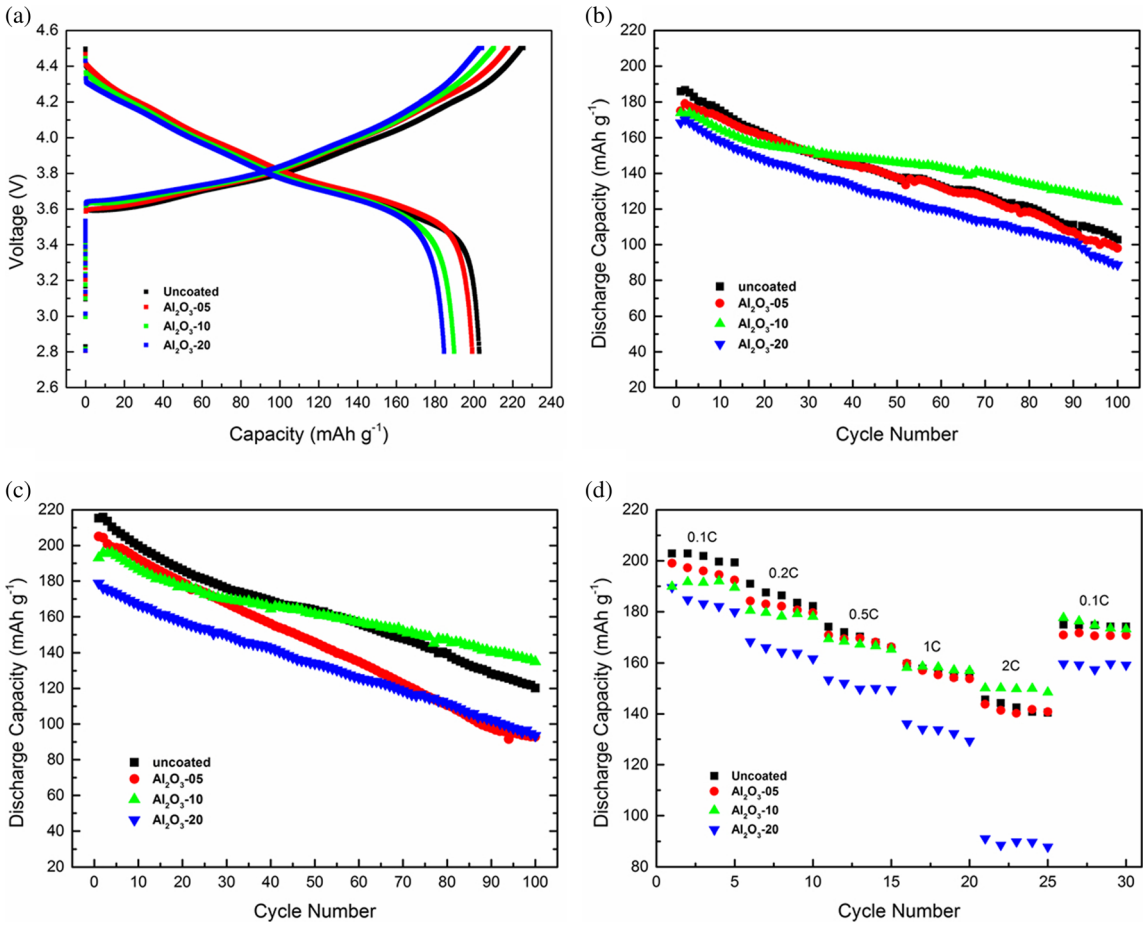

Fig. 5 Electrochemical properties: initial charge/discharge curves of the uncoated and Al_2O_3-coated $LiNi_{0.8}Co_{0.15}Al_{0.05}O_2$ at a current density of 18 mA g^{-1} (0.1C) over the voltage range of 2.8–4.5 V (**a**), cycle performance at the current rate of 1C at room temperature (25 °C) (**b**), cycle performance at the current rate of 1C at elevated temperature (55 °C) (**c**), and rate capability test of the Li/uncoated and Li/Al_2O_3-coated $LiNi_{0.8}Co_{0.15}Al_{0.05}O_2$ cells as a function of C rate (**d**)

185.78 to 102.76 mAh g^{-1} and 215.24 to 120.24 mAh g^{-1} at the rate of 1C after 100 cycles and shows a capacity retention rate of 55.3 and 55.8 %, respectively; 1-wt.% Al_2O_3-coated $LiNi_{0.8}Co_{0.15}Al_{0.05}O_2$ cells provide a higher capacity retention of 71.7 % (173.94 to 124.71 mAh g^{-1}) and 70.1 % (193.06 to 135.34 mAh g^{-1}) at 25 and 55 °C after the same cycles, by contrast; 0.5- and 2-wt.% Al_2O_3-coated $LiNi_{0.8}Co_{0.15}Al_{0.05}O_2$ cells show no improvements in electrochemical characters because the amounts of Al_2O_3 are too small and large. Too thin or thick coating layer will have no effect of protecting the anode or impede transmission of ions. This remarkable improvement is mainly due to the dense Al_2O_3 coated on the surface which acts as a physical barrier protecting coated materials from HF attack, reduces side reactions between the electrode and the electrolyte, and provides a more stable electrode/electrolyte interface. Besides, 1-wt.% Al_2O_3-coated $LiNi_{0.8}Co_{0.15}Al_{0.05}O_2$ cells also show better discharge capacity retentions during cycling at higher current densities (1C and 2C).

The electrochemical impedance spectroscopy (EIS) measurement was carried out after 50 charge–discharge cycles at 1C to elucidate changes in electrochemical performance after the Al_2O_3 coating. Nyquist plots of the uncoated and Al_2O_3-coated $LiNi_{0.8}Co_{0.15}Al_{0.05}O_2$ electrodes are shown in Fig. 6. The semicircle in the high-to-medium frequency region is ascribed to the surface impedance (Rf) of Li^+ diffusion in the surface layer; the other in the medium frequency region is assigned to the charge transfer resistance (Rct). [31–33]. Equivalent circuit matches with the curve, and the values of solution resistance (Rs), surface resistance (Rf), and charge transfer resistance (Rct) are as listed in Table 1. The lower Rf and Rct are attributed to a more stable surface protected by Al_2O_3 coating which can suppress the increasing impedance and favor the lithium diffusion of the host oxide during the charge–discharge process [34].

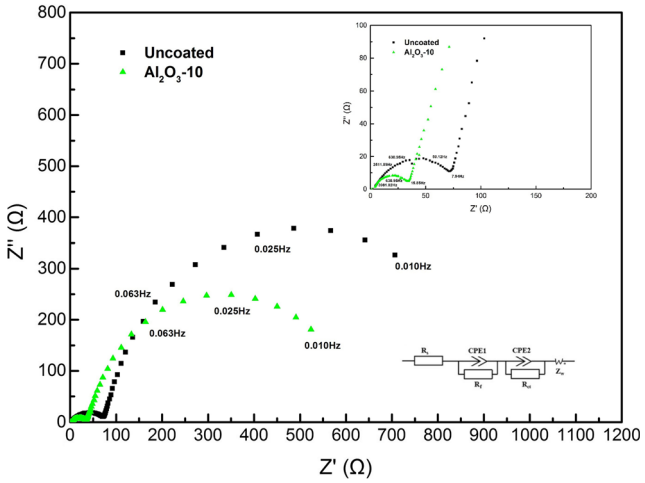

Fig. 6 Nyquist plots of the uncoated and Al_2O_3-coated $LiNi_{0.8}Co_{0.15}Al_{0.05}O_2$ electrodes after 50 charge–discharge cycles

Table 1 Fitting values of the Rs, Rf, and Rct based on the equivalent circuit in Fig. 6

Samples	Rs	Rf	Rct
Uncoated	2.677	79.99	910.5
Al_2O_3-10	3.44	29.97	639.8

Conclusion

In this paper, Al_2O_3 was successfully coated on layered Ni-rich $LiNi_{0.8}Co_{0.15}Al_{0.05}O_2$ material. A thin coating layer with 7 nm was formed on the surface. The Al_2O_3-coated $LiNi_{0.8}Co_{0.15}Al_{0.05}O_2$ materials show improved cycling performance at the current rate of 1C over the voltage range of 2.8–4.5 V. This coating layer acts as a physical barrier protecting coated materials from HF attack, reduces side reactions between the electrode and the electrolyte, and forms a more stable SEI layer. Al_2O_3-coated $LiNi_{0.8}Co_{0.15}Al_{0.05}O_2$ synthesized by a facile method with improved cycling performance presents great potential to be applied in the large-scale energy storage systems (ESSs).

Acknowledgments This research was supported by the Jiangsu Province Prospective Joint Research on Pilot Project (No. BY2013072-03), a Grant for State Key Program for Basic Research of China (Nos. 2013CB632702 and 2012CB921503), the National Natural Science Foundation of China (No. 11134006), a project funded by the Priority Academic Program Development of Jiangsu Higher Education Institutions (PAPD), a project of free exploration funded by the National Laboratory of Solid State Microstructures, Test Foundation of Nanjing University.

References

1. Bang HJ, Joachin H, Yang H, Amine K, Prakash J (2006) Contribution of the structural changes of LiNi0.8Co0.15Al0.05O2 cathodes on the exothermic reactions in Li-ion cells. J Electrochem Soc 153(4):A731–A737. doi:10.1149/1.2171828
2. Yoon WS, Chung KY, McBreen J, Yang XQ (2006) A comparative study on structural changes of LiCo1/3Ni1/3Mn1/3O2 and LiNi0.8Co0.15Al0.05O2 during first charge using in situ XRD. Electrochem Commun 8(8):1257–1262. doi:10.1016/j.elecom.2006.06.005
3. Kostecki R, McLarnon F (2004) Local-probe studies of degradation of composite LiNi0.8Co0.15Al0.05O2 cathodes in high-power lithium-ion cells. Electrochem Solid St 7(10):A380–A383. doi:10.1149/1.1793771
4. Zhuang GV, Chen GY, Shim J, Song XY, Ross PN, Richardson TJ (2004) Li2CO3 in LiNi0.8Co0.15Al0.05O2 cathodes and its effects on capacity and power. J Power Sources 134(2):293–297. doi:10.1016/j.jpowsour.2004.02.030
5. Zhang YC, Wang CY (2009) Cycle-life characterization of automotive lithium-ion batteries with LiNiO2 cathode. J Electrochem Soc 156(7):A527–A535. doi:10.1149/1.3126385
6. Myung ST, Cho MH, Hong HT, Kang TH, Kim CS (2005) Electrochemical evaluation of mixed oxide electrode for Li-ion secondary batteries: Li(1.1)Mn(1.9)O(4)and LiNi0.8Co0.15Al0.05O2. J

Power Sources 146(1-2):222–225. doi:10.1016/j.jpowsour.2005.03.031
7. Ohzuku T, Ueda A, Nagayama M (1993) Electrochemistry and structural chemistry of Linio2 (R(3)over-Bar-M) for 4 volt secondary lithium cells. J Electrochem Soc 140(7):1862–1870. doi:10.1149/1.2220730
8. Itou Y, Ukyo Y (2005) Performance of LiNiCoO2 materials for advanced lithium-ion batteries. J Power Sources 146(1-2):39–44. doi:10.1016/j.jpowsour.2005.03.091
9. Andersson AM, Abraham DP, Haasch R, MacLaren S, Liu J, Amine K (2002) Surface characterization of electrodes from high power lithium-ion batteries. J Electrochem Soc 149(10):A1358–A1369. doi:10.1149/1.1505636
10. Arai H, Tsuda M, Saito K, Hayashi M, Sakurai Y (2002) Thermal reactions between delithiated lithium nickelate and electrolyte solutions. J Electrochem Soc 149(4):A401–A406. doi:10.1149/1.1452114
11. Aurbach D (2000) Review of selected electrode-solution interactions which determine the performance of Li and Li ion batteries. J Power Sources 89(2):206–218. doi:10.1016/S0378-7753(00)00431-6
12. Oh Y, Ahn D, Nam S, Park B (2010) The effect of Al2O3-coating coverage on the electrochemical properties in LiCoO2 thin films. J Solid State Electr 14(7):1235–1240. doi:10.1007/s10008-009-0946-7
13. Thackeray MM, Johnson CS, Kim JS, Lauzze KC, Vaughey JT, Dietz N, Abraham D, Hackney SA, Zeltner W, Anderson MA (2003) ZrO2- and Li2ZrO3-stabilized spinel and layered electrodes for lithium batteries. Electrochem Commun 5(9):752–758. doi:10.1016/S1388-2481(03)00179-6
14. Myung ST, Izumi K, Komaba S, Sun YK, Yashiro H, Kumagai N (2005) Role of alumina coating on Li-Ni-Co-Mn-O particles as positive electrode material for lithium-ion batteries. Chem Mater 17(14):3695–3704. doi:10.1021/cm050566s
15. Lim SN, Ahn W, Yeon SH, Bin Park S (2014) Enhanced elevated-temperature performance of Li(Ni0.8Co0.15Al0.05)O-2 electrodes coated with Li2O-2B(2)O(3) glass. Electrochim Acta 136:1–9. doi:10.1016/j.electacta.2014.05.056
16. Cho Y, Cho J (2010) Significant improvement of LiNi0.8Co0.15Al0.05O2 cathodes at 60 degrees C by SiO2 dry coating for Li-ion batteries. J Electrochem Soc 157(6):A625–A629. doi:10.1149/1.3363852
17. Lee HJ, Nam SC, Park YJ (2011) Protection effect of ZrO2 coating layer on LiCoO2 thin film. B Korean Chem Soc 32(5):1483–1490. doi:10.5012/bkcs.2011.32.5.1483
18. Hu SK, Cheng GH, Cheng MY, Hwang BJ, Santhanam R (2009) Cycle life improvement of ZrO2-coated spherical LiNi1/3Co1/3Mn1/3O2 cathode material for lithium ion batteries. J Power Sources 188(2):564–569. doi:10.1016/j.jpowsour.2008.11.113
19. Cho Y, Lee YS, Park SA, Lee Y, Cho J (2010) LiNi0.8Co0.15Al0.05O2 cathode materials prepared by TiO2 nanoparticle coatings on Ni0.8Co0.15Al0.05(OH)(2) Precursors. Electrochim Acta 56(1):333–339. doi:10.1016/j.electacta.2010.08.074
20. Xu Y, Li XH, Wang ZX, Guo HJ, Huang B (2015) Structure and electrochemical performance of TiO2-coated LiNi0.80CO0.15Al0.05O2 cathode material. Mater Lett 143:151–154. doi:10.1016/j.matlet.2014.12.093
21. Lee SH, Yoon CS, Amine K, Sun YK (2013) Improvement of long-term cycling performance of Li[Ni0.8Co0.15Al0.05]O-2 by AlF3 coating. J Power Sources 234:201–207. doi:10.1016/j.jpowsour.2013.01.045
22. Hu GR, Deng XR, Peng ZD, Du K (2008) Comparison of AlPO4- and Co-3(PO4)(2)-coated LiNi0.8Co0.2O2 cathode materials for Li-ion battery. Electrochim Acta 53(5):2567–2573. doi:10.1016/j.electacta.2007.10.040
23. Wang JP, Du CY, Yan CQ, He XS, Song B, Yin GP, Zuo PJ, Cheng XQ (2015) Al2O3 coated concentration-gradient Li[Ni0.73Co0.12Mn0.15]O-2 cathode material by freeze drying for long-life lithium ion batteries. Electrochim Acta 174:1185–1191. doi:10.1016/j.electacta.2015.06.112
24. Qiu Q, Huang X, Chen YM, Tan Y, Lv WZ (2014) Al2O3 coated LiNi1/3Co1/3Mn1/3O2 cathode material by sol-gel method: preparation and characterization. Ceram Int 40(7):10511–10516. doi:10.1016/j.ceramint.2014.03.023
25. Tang YF, Huang ZP, Feng L, Chen YF (2005) Fabrication of alpha-AlO(OH)center dot SiO2 with core-shell structures by heterogeneous nucleation-and-growth processing. Appl Surf Sci 241(3-4):412–415. doi:10.1016/j.apsusc.2004.07.038
26. Tang YF, Li AD, Lu YN, Li XY, Shi SZ, Ling ZD (2003) Preparation of core/shell structure of alpha-Al(OH)(3)-SiO2 by heterogeneous nucleation-and-growth processing. J Sol-Gel Sci Techn 27(3):263–265. doi:10.1023/A:1024056617029
27. Tang YF, Lu YN, Li AD, Li XY, Shi SZ, Ling ZD (2002) Fabrication of fine mullite powders by alpha-Al(OH)(3)-SiO2 core-shell structure precursors. Appl Surf Sci 202(3-4):211–217. doi:10.1016/S0169-4332(02)00905-4
28. Tang YF, Li AD, Ling HQ, Wang YJ, Shao QY, Lu YN, Ling ZD (2002) Fabrication of composite particles with core-shell structures by a novel processing. J Mater Sci 37(16):3377–3379. doi:10.1023/A:1016597108481
29. Kim MH, Shin HS, Shin D, Sun YK (2006) Synthesis and electrochemical properties of Li[Ni0.8Co0.1Mn0.1]O-2 and Li[Ni0.8Co0.2]O-2 via co-precipitation. J Power Sources 159(2):1328–1333. doi:10.1016/j.jpowsour.2005.11.083
30. Yang SY, Wang XY, Yang XK, Bai YS, Liu ZL, Shu HB, Wei QL (2012) Determination of the chemical diffusion coefficient of lithium ions in spherical Li[Ni0.5Mn0.3Co0.2]O-2. Electrochim Acta 66:88–93. doi:10.1016/j.electacta.2012.01.061
31. Levi MD, Salitra G, Markovsky B, Teller H, Aurbach D, Heider U, Heider L (1999) Solid-state electrochemical kinetics of Li-ion intercalation into Li1-xCoO2: simultaneous application of electroanalytical techniques SSCV, PITT, and EIS. J Electrochem Soc 146(4):1279–1289. doi:10.1149/1.1391759
32. Aurbach D, Levi MD, Levi E, Teller H, Markovsky B, Salitra G, Heider U, Heider L (1998) Common electroanalytical behavior of Li intercalation processes into graphite and transition metal oxides. J Electrochem Soc 145(9):3024–3034. doi:10.1149/1.1838758
33. Zhuang QC, Wei T, Du LL, Cui YL, Fang L, Sun SG (2010) An electrochemical impedance spectroscopic study of the electronic and ionic transport properties of spinet LiMn2O4. J Phys Chem C 114(18):8614–8621. doi:10.1021/jp9109157
34. Zhao X, Zhuang QC, Wu C, Wu K, Xu JM, Zhang MY, Sun XL (2015) Impedance studies on the capacity fading mechanism of Li(Ni0.5Co0.2Mn0.3)O-2 cathode with high-voltage and high-temperature. J Electrochem Soc 162(14):A2770–A2779. doi:10.1149/2.0851514jes